Published in final edited form as:

AJR Am J Roentgenol. 2015 March ; 204(3): W302–W313. doi:10.2214/AJR.14.12733.

Iron-Based Superparamagnetic Nanoparticle Contrast Agents for MRI of Infection and Inflammation

Alexander Neuwelt[1], **Navneet Sidhu**[1], **Chien-An A. Hu**[2], **Gary Mlady**[3], **Steven C. Eberhardt**[3], and **Laurel O. Sillerud**[4]

[1]Department of Internal Medicine, University of New Mexico School of Medicine, Albuquerque, NM

[2]Department of Biochemistry and Molecular Biology, University of New Mexico School of Medicine, Albuquerque, NM

[3]Department of Radiology, University of New Mexico School of Medicine, Albuquerque, NM

[4]UNM BRaIN Center, Department of Neurology, University of New Mexico School of Medicine, 1101 Yale Blvd NE, Albuquerque, NM 87106

Abstract

OBJECTIVE—In this article, we summarize the progress to date on the use of superparamagnetic iron oxide nanoparticles (SPIONs) as contrast agents for MRI of inflammatory processes.

CONCLUSION—Phagocytosis by macrophages of injected SPIONs results in a prolonged shortening of both T2 and T2* leading to hypointensity of macrophage-infiltrated tissues in contrast-enhanced MR images. SPIONs as contrast agents are therefore useful for the in vivo MRI detection of macrophage infiltration, and there is substantial research and clinical interest in the use of SPION-based contrast agents for MRI of infection and inflammation. This technique has been used to identify active infection in patients with septic arthritis and osteomyelitis; importantly, the MRI signal intensity of the tissue has been found to return to its un-enhanced value on successful treatment of the infection. In SPION contrast-enhanced MRI of vascular inflammation, animal studies have shown decreased macrophage uptake in atherosclerotic plaques after treatment with statin drugs. Human studies have shown that both coronary and carotid plaques that take up SPIONs are more prone to rupture and that abdominal aneurysms with increased SPION uptake are more likely to grow. Studies of patients with multiple sclerosis suggest that MRI using SPIONs may have increased sensitivity over gadolinium for plaque detection. Finally, SPIONs have enabled the tracking and imaging of transplanted stem cells in a recipient host.

Keywords

ferumoxytol; infection; inflammation; macrophages; MRI; superparamagnetic iron oxide nanoparticles (SPIONs)

Address correspondence to: L. O. Sillerud (laurel@unm.edu).

After IV injection into humans, superparamagnetic iron oxide nanoparticles (SPIONs) become phagocytosed by macrophages and show prolonged T2 and T2* effects on contrast-enhanced MR images in macrophage-infiltrated tissues [1]. As a result, MRI using SPION-based contrast agents can be considered a biomarker of macrophage infiltration [2]. SPIONs travel to sites of inflammation where their small size of 10–100 nm enables them to leak through permeable capillaries into inflamed tissues where they are taken up by macrophages [3]. Because the effect of SPION uptake by macrophages on MRI has only recently been exploited for the imaging of inflammation and infection, we review both the animal studies that form the basis for our understanding and the subsequent clinical applications of SPIONs that have resulted. We cover the advantages and disadvantages of SPION-enhanced MRI and compare them with the standard gadolinium-enhanced techniques where appropriate and to the techniques in place that use x-rays and gamma rays. Finally, we address the question of the use of iron-based contrast agents in cases of acute or chronic kidney disease and infection.

Macrophages play a central role in both the acute and chronic phases of inflammation. Acutely, macrophages induce the inflammatory reaction required to eradicate an infectious agent, a side effect of which is increased vascular permeability. Acute inflammatory reactions are characterized by a marked infiltration of the tissue by free fluid (edema) accompanied by a cellular infiltration of neutrophils and macrophages [4]. After resolution of the acute infection, macrophages coordinate the repair process, including the creation of a fibrous scar [5]. Chronic infections are characterized histologically by the presence of macrophages and lymphocytes [6]. Applications of MRI to the characterization of chronic infections began with the use of gadolinium-based contrast agents, but this approach was found to have limited specificity [7, 8] because these agents were not taken up by macrophages. Later studies have shown, however, that the use of SPION-based contrast agents resulted in improved accuracy in the MRI depiction of chronic infection, likely because of the important role played by macrophages in the chronic inflammatory process [6]. The ability MRI provides to diagnose and monitor inflammation has important clinical applications because acute tissue changes occur far earlier than tissue necrosis and loss of function. Improved imaging techniques can therefore enable earlier clinical intervention in inflammatory disease and better outcomes [9]. Furthermore, reliable accurate MRI visualization of inflammation can enable non-invasive longitudinal monitoring of disease and treatment efficacy [10].

MRI excels at imaging inflammation because of its high spatial resolution (~0.1–1 mm), ability to depict soft tissues and free fluid, and lack of ionizing radiation, unlike CT or PET. This benefit was highlighted in a recent study that showed the ability of SPI-ON contrast-enhanced MRI to stage pediatric malignancies as accurately as PET/CT using ^{18}F-FDG without the need for ionizing radiation [11] (Fig. 1). A potential drawback of MRI is longer image acquisition times (on the order of minutes), leading to greater motion sensitivity unless modern rapid sequences are used. Also, the low intrinsic sensitivity of nuclear magnetism means that tissue concentrations of MRI probes must be in the micro- to millimolar range compared with the subnanomolar concentrations of radionuclides required for SPECT or PET/CT [9, 12, 13]. However, like gadolinium-based MRI, SPION-enhanced MRI relies on the paramagnetism of electrons to perturb the relaxation times of abundant

nearby water protons. The larger magnetic moments of SPIONs relative to molecules containing gadolinium explain the increased relaxivity of SPIONs compared with gadolinium at similar tissue concentrations [10].

Some of the drawbacks to SPION imaging are summarized in a study by Storey et al. [14]. For instance, repeated infusions of SPIONs may lead to iron deposition and subsequently elevated iron levels that have the potential to cause tissue damage via oxidative injury. Furthermore, they noted a wide variation in iron clearance rates; 50% of the subjects required up to 11 months to eliminate the excess iron from the body (Fig. 2). As a result, SPION agents may affect signal contrast on subsequent radiographic examinations of up to several months later, for example, in the liver. Iron also has a high magnetic susceptibility, and this deposition in turn may lead to MR image artifacts [14]. Despite these potential prolonged changes in the MRI signal intensity, we are aware of no evidence that focal lesions have been masked as a result of earlier SPION administration, and it seems likely that if radiologists are aware that a patient recently received SPIONs, the quality of the image interpretation would not be compromised. Furthermore, it is unclear that the persistent signal intensity changes on the iron-specific sequences used by Storey et al. are secondary to SPION activity and not a result of increased iron stores [14]. For instance, significant changes on T2-weighted images have been observed 3 months after the IV administration of non-SPIONs [15]. Prolonged MRI contrast changes in other organs, such as the spleen, are less likely to be an issue because the duration of altered MRI signals is significantly shorter in these organs than in the liver [14].

SPIONs for Imaging Infection in Animals

SPION-based contrast agents have shown promising results in animal studies for MRI of infections. For example, studies by Lefevre et al. [16] have shown a marked MR signal intensity loss in the septic knees of rabbits injected with SPIONs [16] (Fig. 3). The degree of T2-weighted signal intensity loss in SPION-treated subjects was found to correlate with the iron content in the imaged area [17]. Furthermore, Bierry et al. [2] showed that gadolinium alone was unable to distinguish osteomyelitis from sterile inflammation induced by mechanical damage in rabbit vertebral osteomyelitis, but SPIONs were effective for this purpose [2]. This distinction could be made because macrophages are relatively sparse in areas of noninfectious degenerative change [18, 19].

The successful use of SPION-based contrast agents in the MRI of osteomyelitis is based on the massive infiltration of inflammatory cells, including macrophages, triggered by bone infection [20]. Macrophages were seen to infiltrate the bone marrow in rabbits with vertebral osteomyelitis, which was visualized with SPION-enhanced MRI [2]. Gadolinium-enhanced MRI, by contrast, was unable to differentiate osteomyelitis from sterile inflammation in this study. A second study similarly showed an altered MRI signal-to-noise ratio on SPION-enhanced MRI in rabbits with histologically confirmed osteomyelitis 24 hours after SPI-ON administration [21].

Another important potential application for SPIONs is to distinguish between cancerous tumors and infectious masses (abscesses). This can be a challenging distinction within the

abdomen, where both entities show increased vascularity and occasionally similar appearances on contrast-enhanced MRI. Seyfer et al. [22] found that abscesses could be differentiated from viable tumor because they displayed a smaller contrast-to-noise ratio than neoplasia when imaged using a T2*-weighted MRI sequence with SPIONs [22]. That this distinction was due to macrophage infiltration into the abscesses was shown using histologic staining of macrophage-associated iron with Prussian blue [22].

SPIONs for the Imaging of CNS Inflammation in Animals

Experimental applications of SPION-enhanced MRI to the imaging of CNS inflammation have grown in the past several years and was summarized in a 2010 article by Stoll and Bendszus [10]. Since that time, SPIONs have been used to image neuroinflammation in an animal model of multiple sclerosis (experimental autoimmune encephalitis [EAE]). Spatiotemporal aspects of neuroimaging in EAE were described by Chin et al. [23] and Baeten et al. [24]. In addition, Thorek et al. [25] used a mouse model of dorsal root injury to show that mice bearing cervical nerve injuries display distinctive enhancement patterns on SPION-enhanced MRI. These findings in experimental animal models suggest that SPION-enhanced MRI has the potential to show neuroinflammation and therefore may have utility in identification of causes of idiopathic back pain.

The earliest applications of SPIONs used nanoparticles coated with a biocompatible surface layer to prolong circulation time but otherwise remained unmodified. However, more recent effort has been directed toward attaching recognition ligands to SPIONs to increase the specificity of their binding to and interactions with biologic targets in the body. For instance, iron oxide nanoparticles conjugated to vascular cell adhesion molecule 1 (VCAM-1) have been used to enhance MRI of both neuroinflammation and acute cerebral ischemia [26, 27]. Similarly, our group has conjugated SPIONs to antibodies against amyloid in Alzheimer disease plaques to enhance MRI detection of the plaques [28]. We have more recently developed iron-platinum (Fe-Pt) nanoparticles [29] that target ionized calcium binding adaptor molecule 1 (Iba-1) on activated cerebral microglia to directly reveal neuroinflammation.

The involvement of macrophages in the repair process after transient occlusion of a cerebral vessel has been monitored using MRI with SPION contrast agents in vivo and confirmed with histology [30]. Cerebral ischemia is known to invoke an inflammatory response, and SPION-associated MR signal intensity changes are related to the detection of inflammatory cells in ischemic areas 3–4 days after the initial insult. However, within the first 24 hours of middle cerebral artery occlusion, SPION-induced MRI changes are related to blood–brain barrier defects and intravascular trapping of the contrast agent by thrombotic vessel occlusion and not by macrophage uptake itself [12, 31, 32].

Other Applications of Using SPIONs to Image Inflammation in Animals

Floc’h et al. [33] used SPIONs to aid the imaging of lipopolysaccharide-induced cochlear inflammation in guinea pigs and showed decreased signal intensity in T2-weighted MR images. A similar study used a turpentine-induced inflammatory model in mice to image murine inflammation by means of SPION-enhanced MRI. This study concluded, in

agreement with findings from human studies, that the optimal timing of contrast-enhanced MRI is 24 hours after administration of SPIONs [34].

Stem cell transplantation is being investigated as an approach for the treatment of knee arthritis, a highly prevalent problem in the United States. Ferumoxytol has been studied as a contrast agent for monitoring the successful engraftment of stem cells and to monitor the development of complications, such as tumor formation or graft rejection. Khurana et al. [35] showed that ferumoxytol could be injected IV into stem cell transplant donors. The in vivo labeled stem cells were confirmed to contain ferumoxytol by histology and were then transplanted into osteochondral defects of stem cell recipient mice. This procedure enabled contrast-enhanced MRI of the stem cells up to 4 weeks after transplantation [35, 36]. Additional studies on MRI of stem cells have been reviewed elsewhere [37].

MRI of renal inflammation with the aid of SPIONs has also been shown. Nontargeted SPIONs were found to be effective in revealing macrophage accumulation in kidney disease [38, 39]. Serkova et al. [39] tested both nontargeted SPIONs and nanoparticles conjugated with a recombinant protein containing the C3d-binding region of the complement receptor type 2 (CR2) for their ability to enhance MR images of a mouse model (MRL/lpr, Jackson Laboratory) of lupus nephritis. Use of the targeted SPIONs led to decreased water T2 in the MRL/lpr mice but not in the wild type (C57LB/6, Jackson Laboratory) mice, and the nontargeted SPIONs did not alter the water signal intensity when used to image the knockout mice (Jackson Laboratory) [39]. This imaging technique shows potential clinical utility for noninvasive monitoring of disease activity in patients with lupus nephritis.

Multiple studies have used SPION-based MRI to detect vascular inflammation [34]. Millon et al. [40] used SPIONs to document the decreased macrophage infiltration in the aortic walls of rabbits after 6 months of a chow diet and treatment with atorvastatin. Ruehm et al. [3] similarly found an altered vascular signal in hyperlipidemic rabbits with atherosclerosis on SPION-enhanced MRI [3]. Yu et al. [41] used SPIONs to detect vascular inflammation in rabbits after percutaneous coronary intervention, with results that were confirmed by histology. In a similar vein, research using an ApoE knockout mouse model ($ApoE^{-/-}$, Jackson Laboratory) has shown convincing detection of inflammatory atherosclerosis by means of SPION-enhanced MRI [42, 43].

Obesity is known to induce inflammation in adipose tissue. Obesity-related macrophage infiltration is thought to contribute to obesity-related comorbidities. Nontargeted SPIONs have been used to show macrophage infiltration of adipose tissue in vivo in ob/ob mice, thereby noninvasively showing adipocyte inflammation [44].

Ferumoxytol for Imaging of Inflammation

Ferumoxytol is the only SPION approved by the Food and Drug Administration (FDA) for human use in the United States. Specifically, ferumoxytol is approved for the treatment of iron deficiency in patients with renal failure. In the clinical studies that led to FDA approval, 1562 patients with chronic kidney disease were given ferumoxytol. The most common adverse reactions were nausea (3.1%) and dizziness (2.6%). Only three of 1726 patients exposed to ferumoxytol had serious hypersensitivity reactions [45]. There were fewer

adverse events associated with ferumoxytol than with oral iron (package insert, Feraheme, AMAG Pharmaceuticals). The superparamagnetic properties of ferumoxytol have led to its off-label use as an MRI contrast agent in humans, including for MRI of the adrenal glands and kidneys and for arthritis [35, 46, 47]. A prominent early example of the potential of SPIONs for MRI came when Harisinghani et al. [48] used ferumoxtran-10 (Combidex, Advanced Magnetics), an earlier-generation SPION manufactured by the same company that makes ferumoxytol, to accurately identify patients with lymph node metastases in prostate cancer. This study found that the sensitivity of Combidex-enhanced MRI exceeded conventional MRI for this purpose 91% versus 35%.

Human Studies Using SPIONs to Image Infection

Vertebral osteomyelitis has been effectively imaged with SPIONs in human studies. Fukuda et al. [49] found that MRI of bone marrow involved in vertebral osteomyelitis showed a distinct relative enhancement with SPIONs compared with the marrow of healthy control subjects. Bierry et al. [50] also found, using SPION-enhanced MRI, a loss of signal intensity on T2-weighted spinal MRI in patients with vertebral osteomyelitis that was not observed in patients with degenerative disk disease. As mentioned previously, the absence of an MRI signal intensity change in chronic noninfectious inflammation is believed to be due to the lack of macrophage infiltration [50]. In this study, gadolinium was not found to be useful to differentiate aseptic inflammation from spinal osteomyelitis because gadolinium only shows increased vascularity, which occurs in both conditions [8].

We are not aware of any studies using ferumoxytol to image infection in human marrow, but Storey and Arbini [51] studied the characteristics of ferumoxytol uptake and elimination in the bone marrow of human subjects (Fig. 4). These authors concluded that macrophage-specific uptake could be useful for identifying infections and inflammation in the marrow because the small size and longer plasma half-life of ferumoxytol result in improved marrow uptake relative to older-generation iron oxide imaging agents. Once in the marrow, ferumoxytol is rapidly taken up by macrophages, thus potentially providing a mechanism for the imaging of active infection. This group also examined the time course of iron elimination from the bone marrow and found that iron was completely removed after 5 months [51].

Human Studies Using SPIONs to Image Inflammation

SPION-enhanced MRI has been used to detect inflammation in the human cardiovascular system. SPION enhancement was useful in showing the existence of myocardial inflammation after myocardial infarction in both the infarcted and remote regions [52]. It was proposed that the protracted presence of macrophages after infarction, detected through SPION-enhanced MRI, might predict an increased likelihood of clinical heart failure [53]. This would have clinical importance because these patients would merit more aggressive therapeutic interventions. Similarly, multiple studies have explored the use of SPIONs to image myocardial inflammation associated with heart transplantation [54, 55], a technique, that if more widely applied, could potentially reduce the need for invasive biopsies to monitor the viability of the transplanted tissue.

Inflammation within carotid plaques was observed by Sadat et al. [56] using SPION-enhanced MRI. Similar studies have looked at both symptomatic and asymptomatic carotid plaques [57, 58]. It is of interest that a greater quantity of SPIONs is seen in rupture-prone carotid plaques than in more stable lesions, perhaps because these unstable plaques have an increased uptake of macrophages and thus are more inflamed [59, 60]. Treatment with atorvastatin was found to decrease SPION uptake in carotid plaques [61].

Richards et al. [62] showed that aortic aneurysms with increased uptake of SPIONs were more likely to grow. Their findings suggest that SPION-enhanced MRI studies might have potential in determining the need for interventions in aortic aneurysms. Of note, the imaging of atheroma using SPIONs has been more comprehensively reviewed elsewhere [63].

Ferumoxytol injections have also been used to enhance the specificity of MRI of the cardiovascular system. In one such application, Hasan et al. [64] observed increased water MRI signal intensity in the walls of aneurysms after 3 months of aspirin use by patients, suggesting that there was a decreased local iron concentration resulting from a lowered macrophage presence in these areas. Intracranial aneurysms and arteriovenous malformations (AVMs) are inflammatory lesions in which pathophysiology is dependent on macrophage activity. In a recent article, Chalouhi et al. [65] summarized the evidence that intracranial aneurysms with early uptake of ferumoxytol are at increased risk of rupturing. They also provided a proof-of-principle study showing that ferumoxytol-enhanced MRI may be used to assess inflammatory cell burden in AVMs [65] (Fig. 5).

SPION-enhanced MRI was found to provide the ability to distinguish the inflamed pancreas of type 1 diabetes mellitus patients from that of normal control subjects, a finding that was based on the infiltration of the pancreatic islets by macrophages [66]. This observation may support the use of SPIONs for noninvasive MRI monitoring of disease progression or response to therapy (Fig. 6).

Multiple human studies have examined the use of SPIONs for imaging neuroinflammation. Vellinga and colleagues [67] used SPIONs and MRI to image autoimmune inflammation in multiple sclerosis (MS) patients. Impressively, this group found 188 lesions in 14 patients using SPION-enhanced MRI compared with only 44 lesions detected with gadolinium-based contrast agents in this same group of patients. These researchers went on to show that even “normal white matter” showed diffuse inflammation in MS patients [68]. Interestingly, Tourdias et al. [69] showed that MS lesions that enhanced with both gadolinium and SPIONs were larger and more likely to also be found during subsequent imaging 6 months later. This group proposed that the lesions that enhanced with both contrast agents might exhibit a more aggressive evolution [69] (Fig. 7). Stroke is another neuroinflammatory process that has been successfully imaged with SPIONs. In clinical studies, SPION enhancement did not correlate with infarct size, although patients generally had hyperintense signal intensity on T1-weighted imaging and hypointense signals on T2-weighted imaging [70, 71] (Fig. 8). Some patients with infarcts did not show SPION enhancement [10].

An important advantage of SPIONs, which distinguishes them from gadolinium-based MRI contrast agents and iodinated CT contrast agents, is their potential for safe use in patients

with chronic kidney disease. For example, ferumoxytol, as described earlier, has been approved by the FDA for iron replacement in chronic kidney disease patients. Hauger et al. [38] showed the feasibility of using SPION-enhanced MRI to monitor macrophage infiltration in native and transplanted kidneys and in patients with kidney transplant rejection; other contrast agents were contraindicated in these patients.

Renal allografts can malfunction for multiple reasons, many of which include inflammatory processes, such as those arising from an ischemic insult because of a lack of vessel patency. As previously described, conventional contrast agents used for CT angiography and MR angiography (MRA) are typically contraindicated in patients with renal insufficiency. However, Bashir et al. [47] were able to use ferumoxytol-enhanced MRA to observe the renal arteries in transplant patients and to assess vessel patency.

Although many studies have explored the role of ferumoxytol in MRI of inflammation, we are not aware of any human studies that have used ferumoxytol in the imaging of infections. This is surprising given that macrophages take up ferumoxytol and that these cells are prevalent at sites of infection. It would therefore seem appropriate to use ferumoxytol as an MRI agent for imaging infection.

Does IV Iron Increase the Risk of Infection?

A concern regarding the use of SPION-based contrast agents for the diagnosis of infections is the potential for the exacerbation of infection due to the IV administration of iron-based contrast agents. This concern stems from the observation in vitro that iron increases bacterial proliferation [72]. Despite this theoretic concern, recent studies have found no evidence that the use of IV iron compounds actually caused the clinical worsening of infections [73, 74]. In addition, neither of the human studies using SPIONs described earlier noted worsening osteomyelitis or other infectious complications after IV iron administration [49, 50]. Yu et al. [75] used the SPION preparation ferucarbotran to image livers in 109 patients with chronic viral hepatitis and did not report any infectious complications. Additional reports are in consensus that hemodialysis patients supplemented with IV iron do not appear to be at an increased risk of infection [76, 77].

No human studies have specifically evaluated the effect of IV iron on concurrent infection. As a result, the practice of administering IV iron to patients with systemic infection is generally avoided in clinical practice, in large part on the basis of animal studies showing worsening of systemic infections in subjects treated with IV iron [78–80].

Given the paucity of evidence linking the administration of IV iron with increased morbidity in patients with existing infections, we believe that the potential utility of using SPIONs for the imaging of infections should be weighed against any risks on a case-by-case basis. Nevertheless, it seems prudent to propose that imaging patients with widespread systemic infections or sepsis with SPION-based contrast agents should be avoided.

Conclusion

The utility of SPIONs for the imaging of infection and inflammation in human disease states appears promising. Importantly, SPIONs may be safely used in patients with chronic kidney disease for contrast-enhanced MRI studies when there are contraindications to other CT or MRI contrast agents.

Acknowledgments

We thank Meghan Brett for her contribution to this article.

References

1. Lutz AM, Weishaupt D, Persohn E, et al. Imaging of macrophages in soft-tissue infection in rats: relationship between ultrasmall superparamagnetic iron oxide dose and MR signal characteristics. Radiology. 2005; 234:765–775. [PubMed: 15665219]
2. Bierry G, Jehl F, Boehm N, Robert P, Dietemann JL, Kremer S. Macrophage imaging by USPIO-enhanced MR for the differentiation of infectious osteomyelitis and aseptic vertebral inflammation. Eur Radiol. 2009; 19:1604–1611. [PubMed: 19198846]
3. Ruehm SG, Corot C, Vogt P, Kolb S, Debatin JF. Magnetic resonance imaging of atherosclerotic plaque with ultrasmall superparamagnetic particles of iron oxide in hyperlipidemic rabbits. Circulation. 2001; 103:415–422. [PubMed: 11157694]
4. Richie, AC.; Boyd, W. Boyd's textbook of pathology. 9. Philadelphia, PA: Lea & Febiger; 1990. p. 60-82.
5. Sephel, GC.; Woodward, SC. Repair, regeneration, and fibrosis. In: Rubin, DS.; Strayer, DS., editors. Rubin's pathology. 5. Philadelphia, PA: Lippincott Williams & Wilkins; 2007. p. 71-98.
6. Kaim AH, Jundt G, Wischer T, et al. Functional-morphologic MR imaging with ultrasmall superparamagnetic particles of iron oxide in acute and chronic soft-tissue infection: study in rats. Radiology. 2003; 227:169–174. [PubMed: 12615996]
7. Kaim A, Ledermann HP, Bongartz G, Messmer P, Muller-Brand J, Steinbrich W. Chronic post-traumatic osteomyelitis of the lower extremity: comparison of magnetic resonance imaging and combined bone scintigraphy/immunoscintigraphy with radiolabelled monoclonal antigranulocyte antibodies. Skeletal Radiol. 2000; 29:378–386. [PubMed: 10963422]
8. Kaim AH, Gross T, von Schulthess GK. Imaging of chronic posttraumatic osteomyelitis. Eur Radiol. 2002; 12:1193–1202. [PubMed: 11976867]
9. Sargsyan SA, Thurman JM. Molecular imaging of autoimmune diseases and inflammation. Mol Imaging. 2012; 11:251–264. [PubMed: 22554489]
10. Stoll G, Bendszus M. New approaches to neuroimaging of central nervous system inflammation. Curr Opin Neurol. 2010; 23:282–286. [PubMed: 20168228]
11. Klenk C, Gawande R, Uslu L, et al. Ionising radiation-free whole-body MRI versus (18)F-fluorodeoxyglucose PET/CT scans for children and young adults with cancer: a prospective, non-randomised, single-centre study. Lancet Oncol. 2014; 15:275–285. [PubMed: 24559803]
12. Leuschner F, Nahrendorf M. Molecular imaging of coronary atherosclerosis and myocardial infarction: considerations for the bench and perspectives for the clinic. Circ Res. 2011; 108:593–606. [PubMed: 21372291]
13. Makowski MR, Henningsson M, Spuentrup E, et al. Characterization of coronary atherosclerosis by magnetic resonance imaging. Circulation. 2013; 128:1244–1255. [PubMed: 24019445]
14. Storey P, Lim RP, Chandarana H, et al. MRI assessment of hepatic iron clearance rates after US-PIO administration in healthy adults. Invest Radiol. 2012; 47:717–724. [PubMed: 23070094]
15. Ferrari P, Kulkarni H, Dheda S, et al. Serum iron markers are inadequate for guiding iron repletion in chronic kidney disease. Clin J Am Soc Nephrol. 2011; 6:77–83. [PubMed: 20876673]
16. Lefevre S, Ruimy D, Jehl F, et al. Septic arthritis: monitoring with USPIO-enhanced macrophage MR imaging. Radiology. 2011; 258:722–728. [PubMed: 21339348]

17. Sigovan M, Boussel L, Sulaiman A, et al. Rapid-clearance iron nanoparticles for inflammation imaging of atherosclerotic plaque: initial experience in animal model. Radiology. 2009; 252:401–409. [PubMed: 19703881]
18. Coventry MB. Anatomy of the intervertebral disk. Clin Orthop Relat Res. 1969; 67:9–15. [PubMed: 5361201]
19. Modic MT, Masaryk TJ, Ross JS, Carter JR. Imaging of degenerative disk disease. Radiology. 1988; 168:177–186. [PubMed: 3289089]
20. Gillespie WJ, Allardyce RA. Mechanisms of bone degradation in infection: a review of current hypotheses. Orthopedics. 1990; 13:407–410. [PubMed: 2185459]
21. Bierry G, Jehl F, Boehm N, et al. Macrophage activity in infected areas of an experimental vertebral osteomyelitis model: USPIO-enhanced MR imaging—feasibility study. Radiology. 2008; 248:114–123. [PubMed: 18458246]
22. Seyfer P, Pagenstecher A, Mandic R, Klose KJ, Heverhagen JT. Cancer and inflammation: differentiation by USPIO-enhanced MR imaging. J Magn Reson Imaging. 2014; 39:665–672. [PubMed: 23723131]
23. Chin CL, Pai M, Bousquet PF, et al. Distinct spatiotemporal pattern of CNS lesions revealed by USPIO-enhanced MRI in MOG-induced EAE rats implicates the involvement of spino-olivocerebellar pathways. J Neuroimmunol. 2009; 211:49–55. [PubMed: 19346009]
24. Baeten K, Hendriks JJ, Hellings N, et al. Visualisation of the kinetics of macrophage infiltration during experimental autoimmune encephalomyelitis by magnetic resonance imaging. J Neuroimmunol. 2008; 195:1–6. [PubMed: 18177950]
25. Thorek DL, Weisshaar CL, Czupryna JC, Winkelstein BA, Tsourkas A. Superparamagnetic iron oxide-enhanced magnetic resonance imaging of neuroinflammation in a rat model of radicular pain. Mol Imaging. 2011; 10:206–214. [PubMed: 21496449]
26. McAteer MA, Sibson NR, von Zur Muhlen C, et al. In vivo magnetic resonance imaging of acute brain inflammation using microparticles of iron oxide. Nat Med. 2007; 13:1253–1258. [PubMed: 17891147]
27. Hoyte LC, Brooks KJ, Nagel S, et al. Molecular magnetic resonance imaging of acute vascular cell adhesion molecule-1 expression in a mouse model of cerebral ischemia. J Cereb Blood Flow Metab. 2010; 30:1178–1187. [PubMed: 20087364]
28. Sillerud LO, Solberg NO, Chamberlain R, et al. SPION-enhanced magnetic resonance imaging of Alzheimer's disease plaques in AbetaPP/PS-1 transgenic mouse brain. J Alzheimers Dis. 2013; 34:349–365. [PubMed: 23229079]
29. Taylor RM, Sillerud LO. Paclitaxel-loaded iron platinum stealth immunomicelles are potent MRI imaging agents that prevent prostate cancer growth in a PSMA-dependent manner. Int J Nanomedicine. 2012; 7:4341–4352. [PubMed: 22915856]
30. Kim J, Kim DI, Lee SK, Kim DJ, Lee JE, Ahn SK. Imaging of the inflammatory response in re-perfusion injury after transient cerebral ischemia in rats: correlation of superparamagnetic iron oxide-enhanced magnetic resonance imaging with histopathology. Acta Radiol. 2008; 49:580–588. [PubMed: 18568546]
31. Desestret V, Brisset JC, Moucharrafie S, et al. Early-stage investigations of ultrasmall super-paramagnetic iron oxide-induced signal change after permanent middle cerebral artery occlusion in mice. Stroke. 2009; 40:1834–1841. [PubMed: 19286601]
32. Kleinschnitz C, Schutz A, Nolte I, et al. In vivo detection of developing vessel occlusion in photo-thrombotic ischemic brain lesions in the rat by iron particle enhanced MRI. J Cereb Blood Flow Metab. 2005; 25:1548–1555. [PubMed: 15917747]
33. Floc'h JL, Tan W, Telang RS, et al. Markers of cochlear inflammation using MRI. J Magn Reson Imaging. 2014; 39:150–161. [PubMed: 23589173]
34. Matsushita T, Kusakabe Y, Fujii H, Murase K, Yamazaki Y. Inflammatory imaging with ultrasmall superparamagnetic iron oxide. Magn Reson Imaging. 2011; 29:173–178. [PubMed: 20850245]
35. Khurana A, Nejadnik H, Chapelin F, et al. Ferumoxytol: a new, clinically applicable label for stem-cell tracking in arthritic joints with MRI. Nanomedicine (Lond). 2013; 8:1969–1983. [PubMed: 23534832]

36. Khurana A, Chapelin F, Beck G, et al. Iron administration before stem cell harvest enables MR imaging tracking after transplantation. Radiology. 2013; 269:186–197. [PubMed: 23850832]
37. Bulte JW. Science to practice: can macrophage infiltration serve as a surrogate marker for stem cell viability? Radiology. 2012; 264:619–620. [PubMed: 22919033]
38. Hauger O, Grenier N, Deminere C, et al. USPIO-enhanced MR imaging of macrophage infiltration in native and transplanted kidneys: initial results in humans. Eur Radiol. 2007; 17:2898–2907. [PubMed: 17929025]
39. Serkova NJ, Renner B, Larsen BA, et al. Renal inflammation: targeted iron oxide nanoparticles for molecular MR imaging in mice. Radiology. 2010; 255:517–526. [PubMed: 20332377]
40. Millon A, Dickson SD, Klink A, et al. Monitoring plaque inflammation in atherosclerotic rabbits with an iron oxide (P904) and (18)F-FDG using a combined PET/MR scanner. Atherosclerosis. 2013; 228:339–345. [PubMed: 23582588]
41. Yu Z, Geng J, Tan Y, Wang Q, Zhu J, Zhang M. Non-invasive assessment of acute vascular inflammation after PCI using USPIO enhanced MRI in vivo. Int J Cardiol. 2011; 151:110–112. [PubMed: 21715029]
42. Michalska M, Machtoub L, Manthey HD, et al. Visualization of vascular inflammation in the atherosclerotic mouse by ultrasmall superparamagnetic iron oxide vascular cell adhesion molecule-1-specific nanoparticles. Arterioscler Thromb Vasc Biol. 2012; 32:2350–2357. [PubMed: 22879583]
43. Burtea C, Ballet S, Laurent S, et al. Development of a magnetic resonance imaging protocol for the characterization of atherosclerotic plaque by using vascular cell adhesion molecule-1 and apoptosis-targeted ultrasmall superparamagnetic iron oxide derivatives. Arterioscler Thromb Vasc Biol. 2012; 32:e36–e48. [PubMed: 22516067]
44. Luciani A, Dechoux S, Deveaux V, et al. Adipose tissue macrophages: MR tracking to monitor obesity-associated inflammation. Radiology. 2012; 263:786–793. [PubMed: 22523321]
45. McCormack PL. Ferumoxytol: in iron deficiency anaemia in adults with chronic kidney disease. Drugs. 2012; 72:2013–2022. [PubMed: 22994536]
46. Gunn AJ, Seethamraju RT, Hedgire S, Elmi A, Daniels GH, Harisinghani MG. Imaging behavior of the normal adrenal on ferumoxytol-enhanced MRI: preliminary findings. AJR. 2013; 201:117–121. [PubMed: 23789664]
47. Bashir MR, Jaffe TA, Brennan TV, Patel UD, Ellis MJ. Renal transplant imaging using magnetic resonance angiography with a nonnephrotoxic contrast agent. Transplantation. 2013; 96:91–96. [PubMed: 23680931]
48. Harisinghani MG, Barentsz J, Hahn PF, et al. Noninvasive detection of clinically occult lymphnode metastases in prostate cancer. N Engl J Med. 2003; 348:2491–2499. [PubMed: 12815134]
49. Fukuda Y, Ando K, Ishikura R, et al. Superparamagnetic iron oxide (SPIO) MRI contrast agent for bone marrow imaging: differentiating bone metastasis and osteomyelitis. Magn Reson Med Sci. 2006; 5:191–196. [PubMed: 17332709]
50. Bierry G, Jehl F, Holl N, et al. Cellular magnetic resonance imaging for the differentiation of infectious and degenerative vertebral disorders: preliminary results. J Magn Reson Imaging. 2009; 30:901–906. [PubMed: 19787738]
51. Storey P, Arbini AA. Bone marrow uptake of ferumoxytol: A preliminary study in healthy human subjects. J Magn Reson Imaging. 2014; 39:1401–1410. [PubMed: 24123697]
52. Alam SR, Shah AS, Richards J, et al. Ultrasmall superparamagnetic particles of iron oxide in patients with acute myocardial infarction: early clinical experience. Circ Cardiovasc Imaging. 2012; 5:559–565. [PubMed: 22875883]
53. Weissleder R, Nahrendorf M, Pittet MJ. Imaging macrophages with nanoparticles. Nat Mater. 2014; 13:125–138. [PubMed: 24452356]
54. Christen T, Nahrendorf M, Wildgruber M, et al. Molecular imaging of innate immune cell function in transplant rejection. Circulation. 2009; 119:1925–1932. [PubMed: 19332470]
55. Wu YL, Ye Q, Sato K, Foley LM, Hitchens TK, Ho C. Noninvasive evaluation of cardiac allograft rejection by cellular and functional cardiac magnetic resonance. JACC Cardiovasc Imaging. 2009; 2:731–741. [PubMed: 19520344]

56. Sadat U, Howarth SP, Usman A, Tang TY, Graves MJ, Gillard JH. Sequential imaging of asymptomatic carotid atheroma using ultrasmall superparamagnetic iron oxide-enhanced magnetic resonance imaging: a feasibility study. J Stroke Cerebrovasc Dis. 2013; 22:e271–e276. [PubMed: 22841932]
57. Howarth SP, Tang TY, Trivedi R, et al. Utility of USPIO-enhanced MR imaging to identify inflammation and the fibrous cap: a comparison of symptomatic and asymptomatic individuals. Eur J Radiol. 2009; 70:555–560. [PubMed: 18356000]
58. Tang TY, Howarth SP, Miller SR, et al. Comparison of the inflammatory burden of truly asymptomatic carotid atheroma with atherosclerotic plaques in patients with asymptomatic carotid stenosis undergoing coronary artery bypass grafting: an ultrasmall superparamagnetic iron oxide enhanced magnetic resonance study. Eur J Vasc Endovasc Surg. 2008; 35:392–398. [PubMed: 18171628]
59. Trivedi RA, Mallawarachi C, U-King-Im JM, et al. Identifying inflamed carotid plaques using in vivo USPIO-enhanced MR imaging to label plaque macrophages. Arterioscler Thromb Vasc Biol. 2006; 26:1601–1606. [PubMed: 16627809]
60. Kooi ME, Cappendijk VC, Cleutjens KB, et al. Accumulation of ultrasmall superparamagnetic particles of iron oxide in human atherosclerotic plaques can be detected by in vivo magnetic resonance imaging. Circulation. 2003; 107:2453–2458. [PubMed: 12719280]
61. Tang TY, Howarth SP, Miller SR, et al. The ATHEROMA (Atorvastatin Therapy: Effects on Reduction of Macrophage Activity) Study: evaluation using ultrasmall superparamagnetic iron oxide-enhanced magnetic resonance imaging in carotid disease. J Am Coll Cardiol. 2009; 53:2039–2050. [PubMed: 19477353]
62. Richards JM, Semple SI, MacGillivray TJ, et al. Abdominal aortic aneurysm growth predicted by uptake of ultrasmall superparamagnetic particles of iron oxide: a pilot study. Circ Cardiovasc Imaging. 2011; 4:274–281. [PubMed: 21304070]
63. Tang TY, Muller KH, Graves MJ, et al. Iron oxide particles for atheroma imaging. Arterioscler Thromb Vasc Biol. 2009; 29:1001–1008. [PubMed: 19229073]
64. Hasan DM, Chalouhi N, Jabbour P, Magnotta VA, Kung DK, Young WL. Imaging aspirin effect on macrophages in the wall of human cerebral aneurysms using ferumoxytol-enhanced MRI: preliminary results. J Neuroradiol. 2013; 40:187–191. [PubMed: 23428244]
65. Chalouhi N, Jabbour P, Magnotta V, Hasan D. The emerging role of ferumoxytol-enhanced MRI in the management of cerebrovascular lesions. Molecules. 2013; 18:9670–9683. [PubMed: 23945642]
66. Gaglia JL, Guimaraes AR, Harisinghani M, et al. Noninvasive imaging of pancreatic islet inflammation in type 1A diabetes patients. J Clin Invest. 2011; 121:442–445. [PubMed: 21123946]
67. Vellinga MM, Oude Engberink RD, Seewann A, et al. Pluriformity of inflammation in multiple sclerosis shown by ultra-small iron oxide particle enhancement. Brain. 2008; 131:800–807. [PubMed: 18245785]
68. Vellinga MM, Vrenken H, Hulst HE, et al. Use of ultrasmall superparamagnetic particles of iron oxide (USPIO)-enhanced MRI to demonstrate diffuse inflammation in the normal-appearing white matter (NAWM) of multiple sclerosis (MS) patients: an exploratory study. J Magn Reson Imaging. 2009; 29:774–779. [PubMed: 19306366]
69. Tourdias T, Roggerone S, Filippi M, et al. Assessment of disease activity in multiple sclerosis phenotypes with combined gadolinium- and super-paramagnetic iron oxide-enhanced MR imaging. Radiology. 2012; 264:225–233. [PubMed: 22723563]
70. Saleh A, Schroeter M, Ringelstein A, et al. Iron oxide particle-enhanced MRI suggests variability of brain inflammation at early stages after ischemic stroke. Stroke. 2007; 38:2733–2737. [PubMed: 17717318]
71. Nighoghossian N, Wiart M, Cakmak S, et al. Inflammatory response after ischemic stroke: a USPIO-enhanced MRI study in patients. Stroke. 2007; 38:303–307. [PubMed: 17170357]
72. Bansal A, Sandhu G, Gupta I, et al. Effect of aggressively driven intravenous iron therapy on infectious complications in end-stage renal disease patients on maintenance hemodialysis. Am J Ther. 2014; 21:250–253. [PubMed: 22832501]

73. Munoz M, Gomez-Ramirez S, Cuenca J, et al. Very-short-term perioperative intravenous iron administration and postoperative outcome in major orthopedic surgery: a pooled analysis of observational data from 2547 patients. Transfusion. 2014; 54:289–299. [PubMed: 23581484]
74. Aronoff GR, Bennett WM, Blumenthal S, et al. Iron sucrose in hemodialysis patients: safety of replacement and maintenance regimens. Kidney Int. 2004; 66:1193–1198. [PubMed: 15327417]
75. Yu JS, Shim JH, Chung JJ, Kim JH, Kim KW. Double contrast-enhanced MRI of viral hepatitis-induced cirrhosis: correlation of gross morphological signs with hepatic fibrosis. Br J Radiol. 2010; 83:212–217. [PubMed: 19505965]
76. Aronoff GR. Safety of intravenous iron in clinical practice: implications for anemia management protocols. J Am Soc Nephrol. 2004; 15(suppl 2):S99–S106. [PubMed: 15585604]
77. Daoud E, Nakhla E, Sharma R. Q: is iron therapy for anemia harmful in the setting of infection? Cleve Clin J Med. 2011; 78:168–170. [PubMed: 21364160]
78. Maynor L, Brophy DF. Risk of infection with intravenous iron therapy. Ann Pharmacother. 2007; 41:1476–1480. [PubMed: 17666575]
79. Robins-Browne RM, Prpic JK. Effects of iron and desferrioxamine on infections with Yersinia enterocolitica. Infect Immun. 1985; 47:774–779. [PubMed: 3972453]
80. Zager RA, Johnson AC, Hanson SY, Lund S. Parenteral iron compounds sensitize mice to injury-initiated TNF-alpha mRNA production and TNF-alpha release. Am J Physiol Renal Physiol. 2005; 288:F290–F297. [PubMed: 15494544]

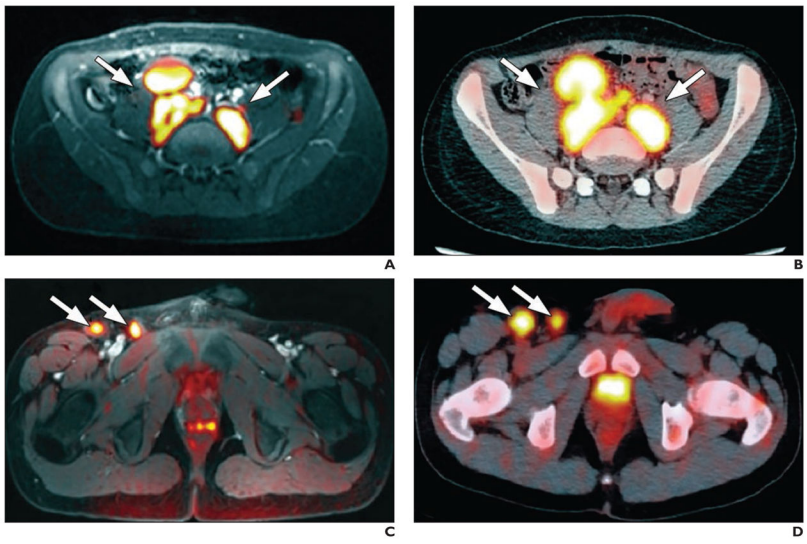

Fig. 1. Hodgkin lymphoma. (Reprinted with permission from [11])

A and **B,** Whole-body diffusion-weighted MR image with ferumoxytol contrast administration (**A**) and FDG PET/CT image (**B**) in 15-year-old patient show positive retroperitoneal involvement (*arrows*) of stage IIIA Hodgkin lymphoma.

C and **D,** Whole-body diffusion-weighted MR image with ferumoxytol contrast administration (**C**) and FDG PET/CT image (**D**) in 14-year-old patient with stage IIB Hodgkin lymphoma show positive right inguinal lymph nodes (*arrows*).

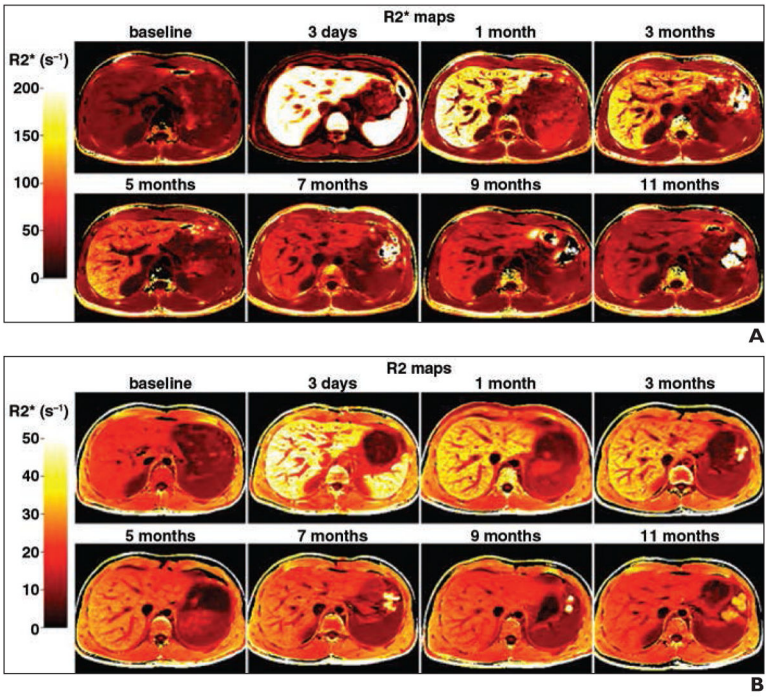

Fig. 2. Relaxometry rate (R2) and effective relaxometry rate (R2*). (Reprinted with permission from [14])

A and **B,** R2* (**A**) and R2 (**B**) images of liver show marked increase in signal at 3 days. In this 28-year-old man, signal intensity for both R2* and R2 did not return to baseline at 11 months. Color scales are shown on left.

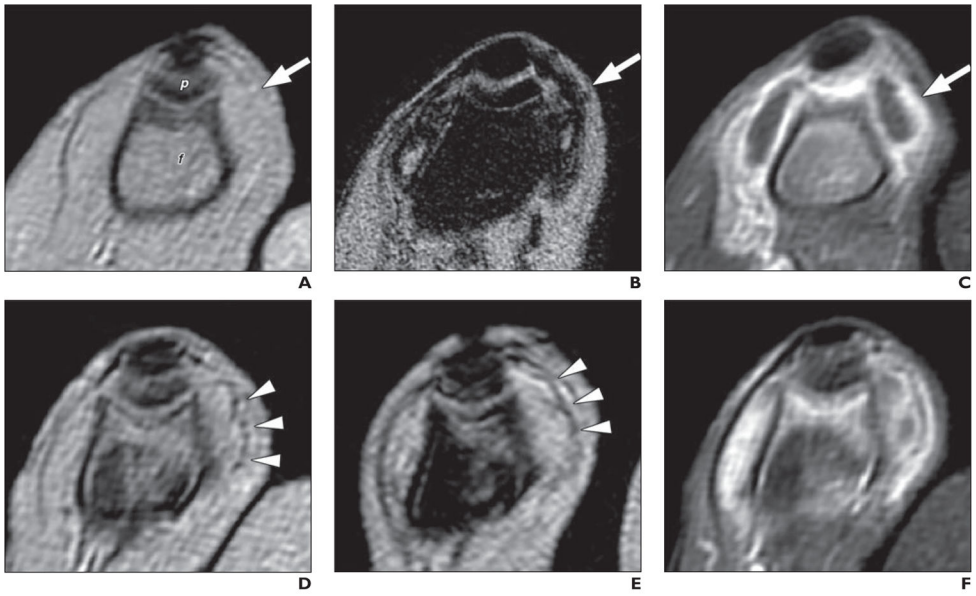

Fig. 3. MRI of septic knee arthritis in rabbit before (A–C) and after (D–F) antibiotic administration. (Adapted and reprinted, with permission from [16])

A, Unenhanced, T2*-weighted image shows thickened synovium (*arrow*). *f* = femur, *p* = patella.

B, T2*-weighted image obtained 24 hours after superparamagnetic iron oxide nanoparticle (SPION) injection shows infiltration of iron-laden macrophages into synovium (*arrow*).

C, Gadolinium-enhanced T1-weighted image shows synovitis (*arrow*).

D, T2*-weighted gradient-echo image shows only focal signal intensity loss in synovium (*arrowheads*).

E, SPION-enhanced MR image after antibiotic administration shows no enhanced signal intensity loss over unenhanced image (*arrowheads*).

F, SPION-enhanced MR image shows gadolinium continues to enhance synovium despite antibiotic treatment.

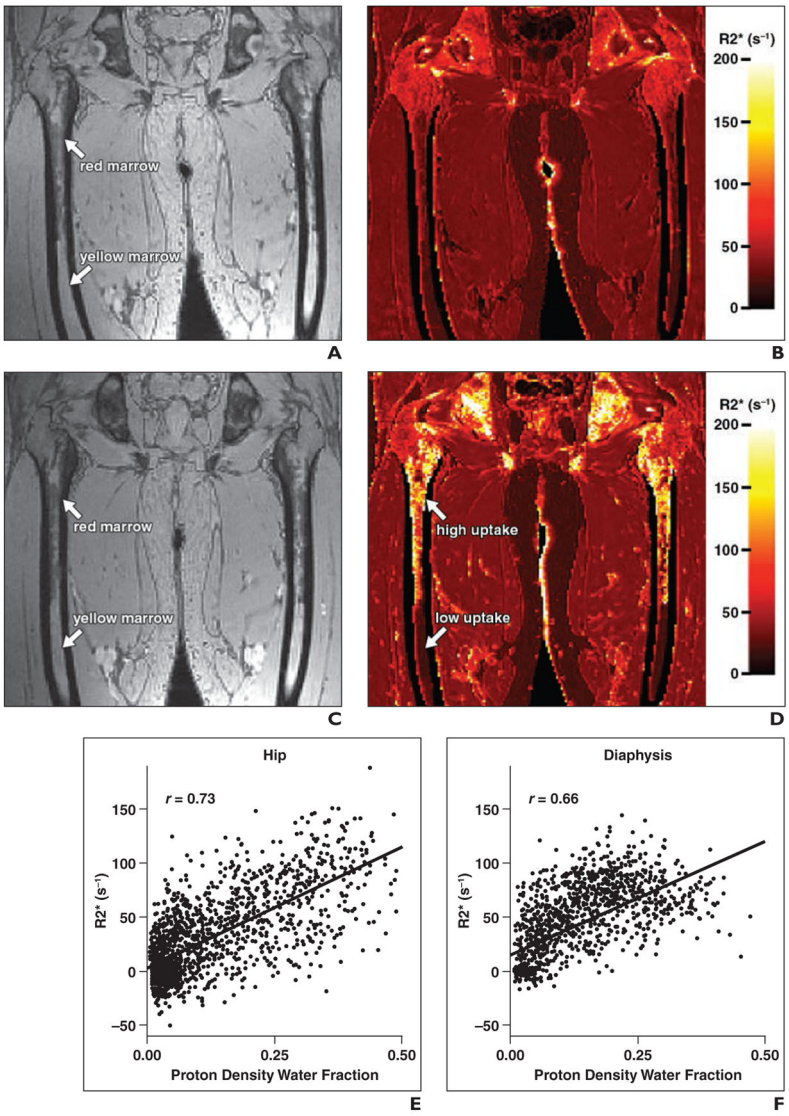

Fig. 4. Hip and femur. (Reprinted with permission from [51])

A–D, Gradient-echo images (**A** and **C**) and effective relaxometry rate (R2*) images (**B** and **D**) show hip and femur of human subjects. **A** and **B** are baseline images and **C** and **D** are images obtained 3 days after ferumoxytol administration. Color scale is provided for R2* maps. In **D**, note that R2* signal intensity with ferumoxytol contrast-enhancement is dramatically increased in red marrow but remains low in yellow marrow. **E** and **F,** Graphs show relation between R2* response and proton density water fraction.

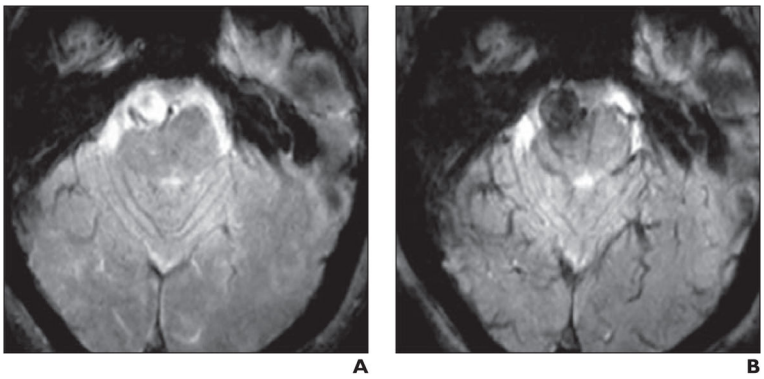

Fig. 5. Patient whose aneurysm ruptured within 3 months. (Adapted and reprinted with permission from [65])

A and **B,** Unenhanced (**A**) and ferumoxytol-enhanced (**B**) images show early uptake of ferumoxytol at 24 hours (**B**) from T2* gradient-recalled echo sequence. This image is from study that suggests that intracranial aneurysms with ferumoxytol uptake within 24 hours are more likely to rupture [65].

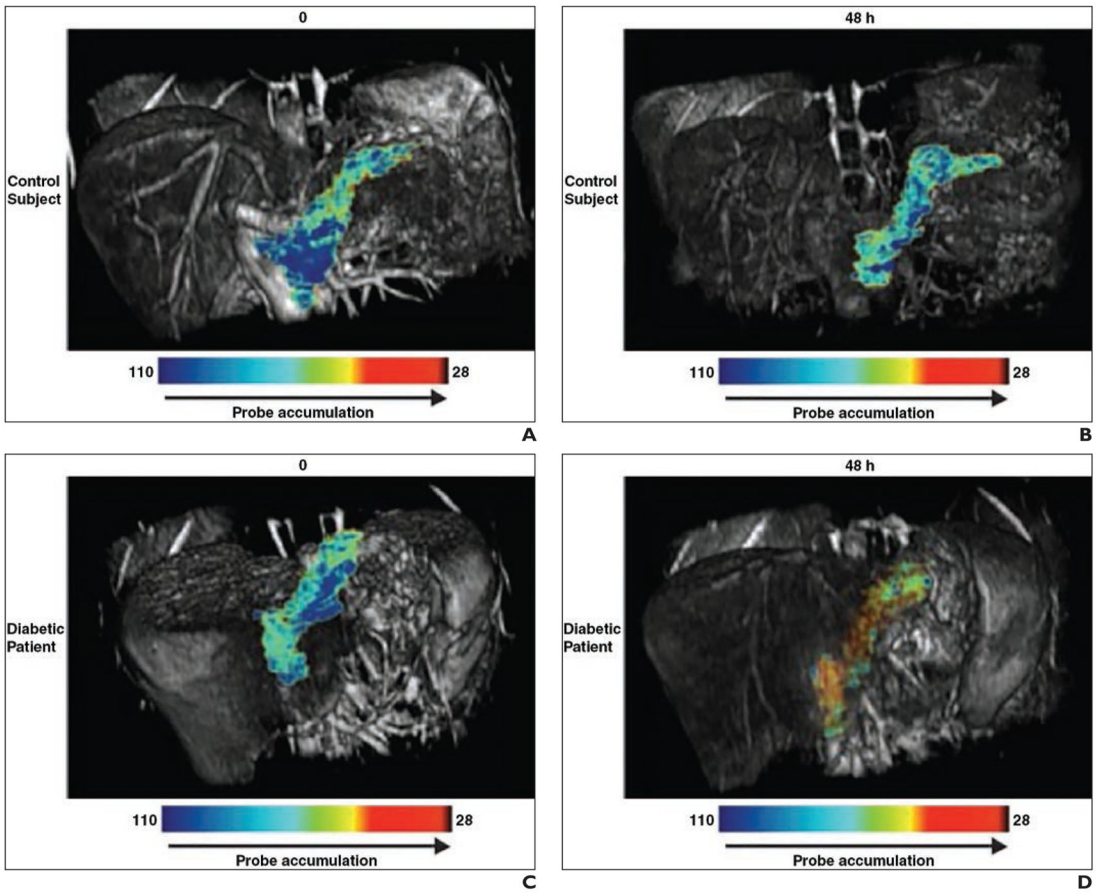

Fig. 6. Diabetes. (Reprinted with permission from [66])

A–D, T2-weighted pseudocolor reconstructions superimposed on unenhanced (**A** and **C**) and superparamagnetic iron oxide nanoparticle (SPION)-enhanced (**B** and **D**) T1-weighted images show no difference between diabetic patients and normal subjects on unenhanced images. However, after ferumoxtran-10 (Combidex, Advanced Magnetics) SPION administration, images are clearly distinct.

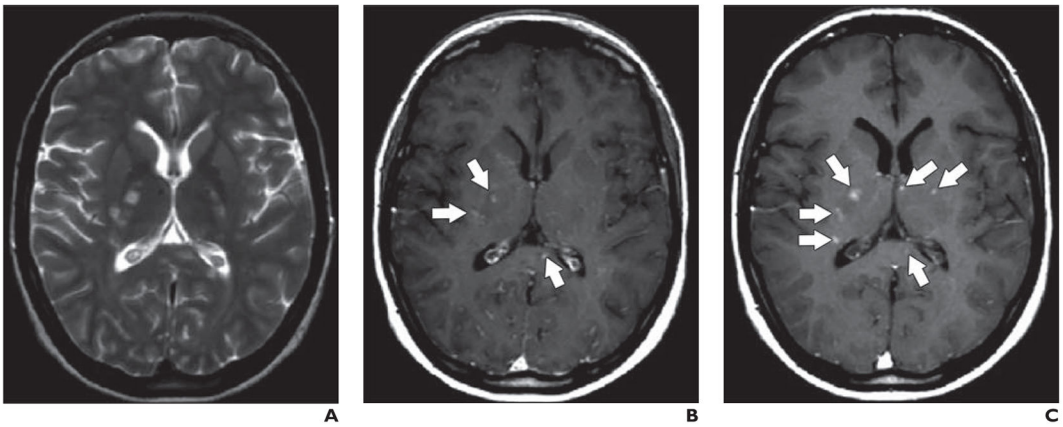

Fig. 7. Multiple sclerosis lesions. (Adapted and reprinted with permission from [69])

A–C, Unenhanced (**A**), gadolinium-enhanced T1-weighted (**B**), and superparamagnetic iron oxide nanoparticle–enhanced (**C**) MR images show multiple sclerosis lesions (*arrows*).

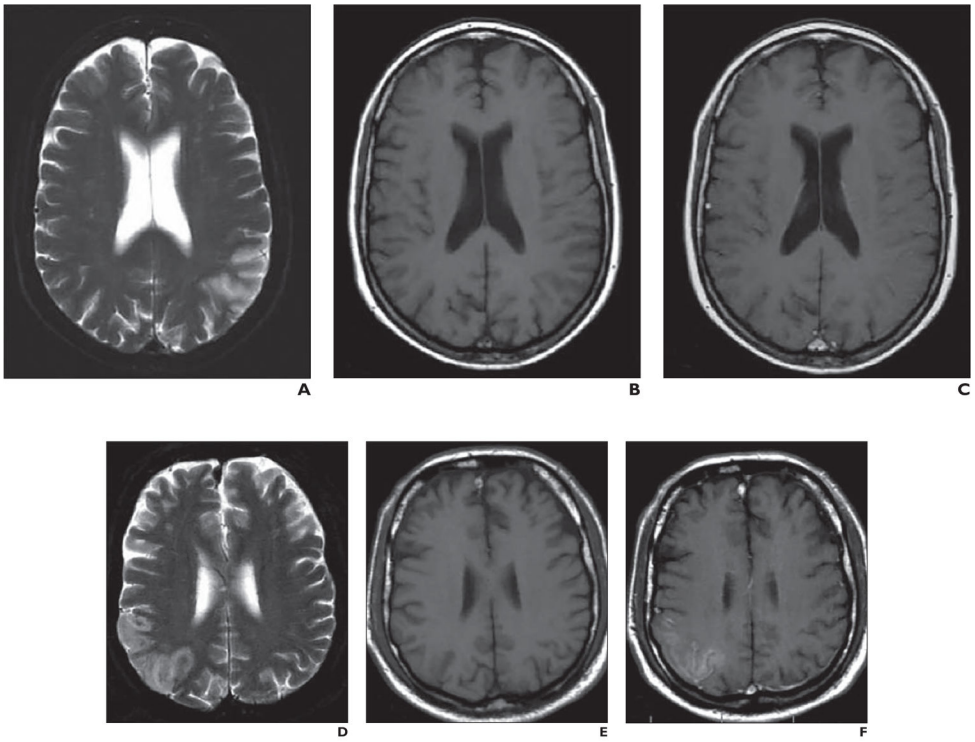

Fig. 8. Comparative analysis of two middle cerebral artery infarctions localized to posterior parietal cortex. (Adapted and reprinted with permission from [70])

A–C, 60-year-old woman 124 hours after stroke onset. T2-weighted image (**A**) shows ischemic lesion. In comparison with unenhanced T1-weighted image (**B**), no enhancement is seen with superparamagnetic iron oxide nanoparticle–enhanced image (**C**).

Comparative analysis of two middle cerebral artery infarctions localized to posterior parietal cortex. (Adapted and reprinted with permission from [70])

D–F, 56-year-old man with infarct imaged 80 hours after stroke onset. Lesion is visualized on T2-weighted image (**D**). Lesion shows improved visualization after ultrasmall superparamagnetic iron oxide infusion (**F**) relative to unenhanced T1-weighted image (**E**).